Transactions on Engineering Sciences vol 32, © 2001 WIT Press, www.witpress.com, ISSN 1743-3533

Forming limit diagram of metal sheet in actual strain path with respect to forming process

M. Shakeri, B.M. Dariani & A.Sadough
Mechanical Engineering Department, Amirkabir University of Technology, Tehran, Iran.

Abstract

Sheet metal forming is generally limited by plastic instability in the form of diffuse necking followed by localized necking and final failure.The forming limit diagram (FLD) is dependent upon the material properties such as strain hardening exponent (n), strain rate sensitivity parameter (m), Anisotropy parameter (r), grain size as well as strain path. Since the actual strain path in the sheet metal forming is not always linear, thus the FLDs that are obtained throughout linear strain path do not have good agreement with experiments. In this paper the FLD of sheet is obtained throughout actual strain path (nonlinear) in both theoretical and experimental approaches. In the theoretical analysis, a localized necking model is used and a "many slices" approach is introduced to assess the FLD. In solving the theoretical formulations, the loading path is considered nonlinear confirming the actual strain path of sheet in the cup drawing. The experimental study is carried out using a special design biaxial tension machine which can produce any strain path on the samples. It is concluded that the limit strains in the actual strain path, near the punch radius in cup drawing, are lower than obtained throughout linear path, the theoretical results show good agreement with experimental results.

1 Introduction

Sheet metal forming is a very important commercial process. Sheet metals are being used increasingly to produce packaging materials, automobile bodies and structural components. Fracture is the major failure in sheet metal forming. The prediction of the forming limit diagram (FLD) of sheet metals is of great importance especially for analysing instabilities and determining the limits of possible deformations in component design.

The FLD, firstly introduced by keeler [1] and Goodwin [2], represents the local limit strains of the sheet metal in the principal strain coordinates. Considerable researches have been carried out on both experimental and theoretical assessment and sensitivity analysis of the FLD. Marciniak and kuczynski [3] developed a theory based on the assumption that necking develops in regions of the initial heterogeneity. Ghosh and Hecker [4] experimentally determined the FLD, using punch test. Priadi and coworkers [5] developed a tensile test on notched specimens to assess the FLD of the sheet metals. Pishbin and Gillis [6] introduced theoretical model for calculation of the FLD, using Hill's nonquadratic flow law for sheets having in-plane isotropy in conjunction with the three-stage deformation approximation. Sing and Rao [7,8] introduced a new method of constructing the FLD by using tensile test results.

The influence of strain-hardening and strain rate sensitivity parameters (n,m) on the strain gradients has been studied by Ghosh [9] and for full-dome formability tests has been investigated by Burford [10]. The authors showed the influence of n,m and Anisotropy parameter (r) on he formability limits of low carbon steel [11]. It is also found that the grain refining annealing improves the formability of the low carbon steel [12].

Some researches also have shown that the FLD is depend on the strain path. Kohara [13], Graf and Husford [14] showed the effect of pre-straining on the formability of aluminum alloy sheets. Shakeri and coworkers [15] studied the effect of uniaxial and biaxial prestraining on the formability of the low carbon steel.

In this paper the forming limit diagram of law carbon steel ST12 in the actual strain path (non linear) is determined and compared with linear strain path.

2 Theoretical analysis

To describe the plastic instability and neck growth, a thin sheet subjected to plane stress state is considered. The analysed material consists of a homogeneous area, labelled by "a" and a heterogeneous area labelled by "b". The defected area is subdivided into slices as shown in figure 1a.

The material is assumed to present orthotropic anisotropy with the principal axes of anisotropy coinciding with the material axes and it obeys Hill's criterion for plane stress state, thus:

$$2h = \sigma_e^{\,2} = (G+H)\,\sigma^{2}_{xx} + (F+H)\,\sigma^{2}_{yy} - 2H\,\sigma_{xx}\,\sigma_{yy} + 2p\sigma^{2}_{xy} \qquad (1)$$

Where F,G,H and P are anisotropic constants. The behaviour of the material can be represented in the form:

$$\sigma_e = c(\varepsilon_0 + \bar{\varepsilon})^{n}\,\dot{\bar{\varepsilon}}^{m} \qquad (2)$$

Where ε_0 is the uniform pre-strain applied to the sample prior to the experiment, ε is the total plastic and c is the strength coefficient.

The equilibrium condition requires that the applied load remains constant along the specimen, so:

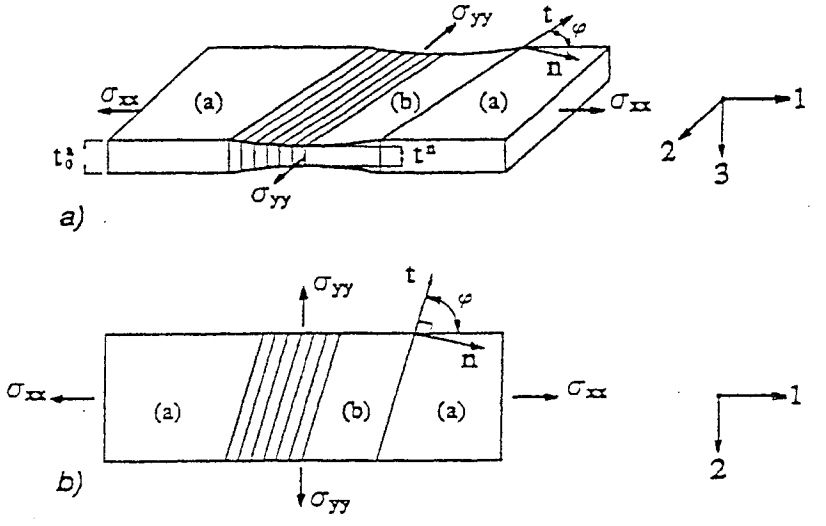

Figure 1: Model of localized necking in theoretical analysis.

$$\sigma_{nn}{}^{a} t^{a} = \sigma_{nn}{}^{b} t^{b} \quad , \sigma_{nt}{}^{a} t^{a} = \sigma_{nt}{}^{b} t^{b} \tag{3}$$

Where the vectors t and n are more clearly shown in figure 1b. The compatibility condition gives

$$d\varepsilon_{tt}{}^{a} = d\varepsilon_{tt}{}^{b} \tag{4}$$

On combining the above equations, the following expression is obtained after a lengthy but straight forward calculation:

$$\frac{d\bar{\varepsilon}^{b}}{d\bar{\varepsilon}^{a}} = \left\{ \frac{(s_1/s_2)^2 T_8}{T_7 f^2 [(\varepsilon_0 + \bar{\varepsilon}^{b}) / (\varepsilon_0 + \bar{\varepsilon}^{a})]^{2n}} \times \left(\frac{d\bar{\varepsilon}^{b}}{d\bar{\varepsilon}^{a}}\right)^{2-2m} - \frac{T_6}{T_7} \right\}^{1/2} \tag{5}$$

More informations about this equation and the parameters, f, T_6, T_7, T_8, s_1 and s_2 are given in ref. [15]

The numerical solution of equation (5) is obtained by iteration with a fourth-order Runge-Kutta method. The loading path for solving this equation is considered non-linear confirming the actual strain path of sheet in the cup drawing. This strain path is shown in figure 2.

In each loading path a finite increment of strain is imposed on region 'a'.By solving equation (5) and knowing the value of the local geometrical defect, it is

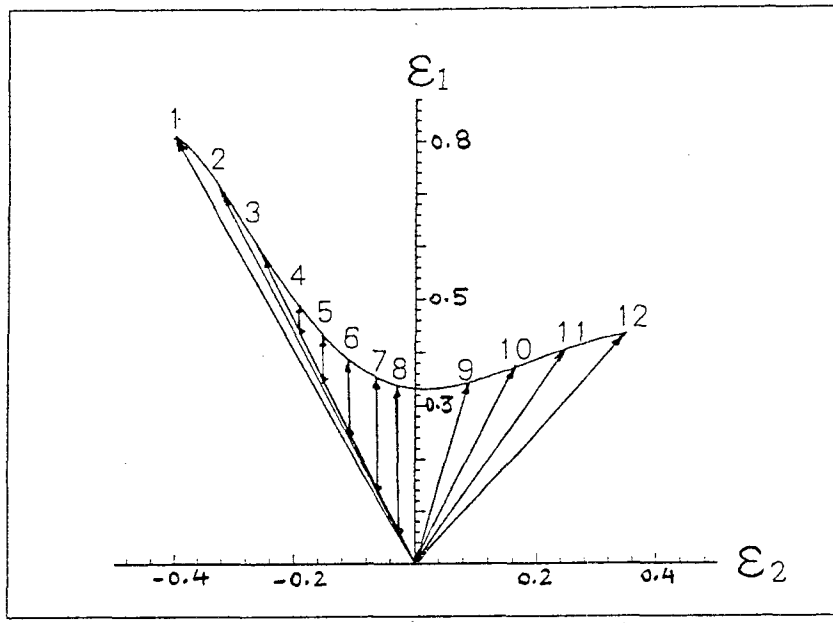

Figure 2: Proper strain path for determination of FLD in the cup drawing.

possible to compute the resultant strain increments in the adjacent slice that is indicated 'b'. The strain states of region 'b' are then used to compute the strain state of the following neighboring slice. The simulation is then repeated until the weakest slice is reached. The numerical computation is performed until $d\bar{\varepsilon}^a / d\bar{\varepsilon}^b < 0.1$ in the full range of strain ratios.

Using this manner, the FLDs are obtained for ST12 low carbon steel in the linear and actual strain path.

3 Experimental procedure

In the experimental study, low carbon steel ST12 (conforming to DIN 1623, No. 1.0330) with 2.5 mm thickness are used. The FLD of ST12 sheets are obtained both in linear and actual strain path according to figure 2.

The FLD of sheet in linear strain path is determined using tension tests and stretch forming tests with a hemispherical punch. The FLD for negative minor strains are determind with notched tensile specimens of various widths. The tensile testing is performed at a crosshead speed of 5 mm/min, using a tensile Instron test machine. The FLD for plane strain and positive minor strains is determind by stretch forming tests with a hemispherical punch of 90 mm diameter, adopting strips of various widths, circular and rectangular blanks.

Transactions on Engineering Sciences vol 32, © 2001 WIT Press, www.witpress.com, ISSN 1743-3533

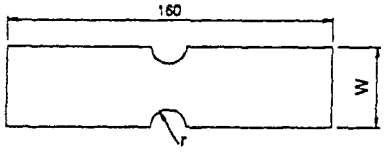

9. Notched tensil specimens with various W and r values.

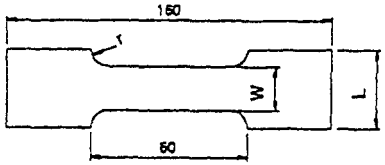

8. Stretch forming strips with various L, W and r values.

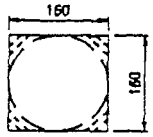

4. Stretch forming circular and rectangular samples.

Figure 3: Notched tensile strip, circular and rectangular stretch forming specimens.

Furthermore various lubricating and non Lubricating conditions are used to realize various strain states.

The geometries of notched tensile specimens and stretch forming strips and blanks are given in figure 3.

The FLD of ST12 sheet in actual strain path (nonlinear) is determind using special tension machine. The drawing of this machine is shown in figure 4. This machine has two hydraulic cylinders and gripers in x direction and two others in y direction and also has a hydraulic cylinder in z direction that activate a hemispherical punch. The nonlinear loading path according to figure 2, can be applied to the samples by adjusting the speeds of the cylinders.

Circular grids of 3 and 4mm diameter are initially printed on the surface of the specimens for the purpose of strain measurement. All tests are continued until a localized necking is achieved. For each specimen the major and minor strain are directly measured from the deformed grids.

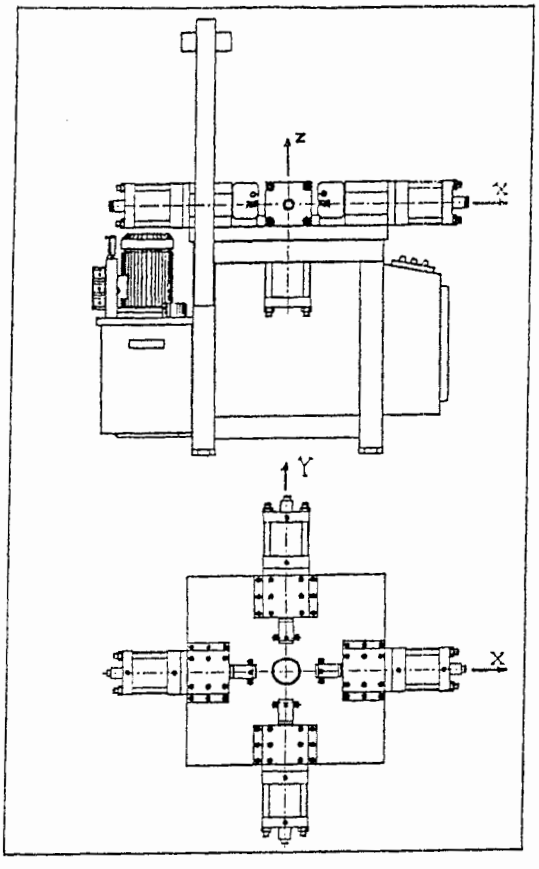

Figure 4: Drawing of special tension machine

4 Results and discussion

The experimental data for theoretical computation of the FLD according to the ST12 sheet properties are as follows:

$n = 0.32$, $m = 0.01$, $r_0 = 2$, $r_{90} = 2.2$

Figure 5 shows the theoretical and experimental FLDs of ST12 sheet in the linear strain path.

In figure 6 the theoretical FLD of ST12 sheet in actual strain path is compared to linear strain path. Figure 7 shows the limit strain in punch radius (cup drawing) that is obtained theoretically in linear and actual strain path and experimentally in actual strain path.

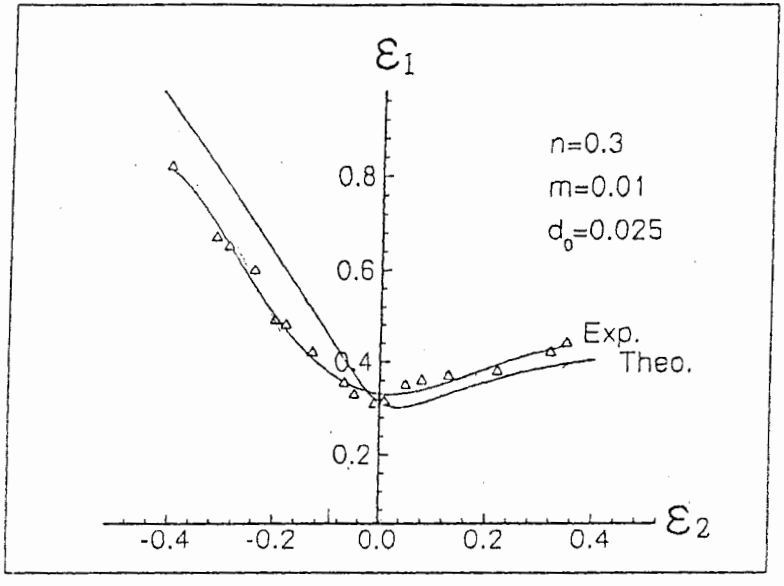

Figure 5: Theoretical and experimental FLDs of ST12 steel sheet

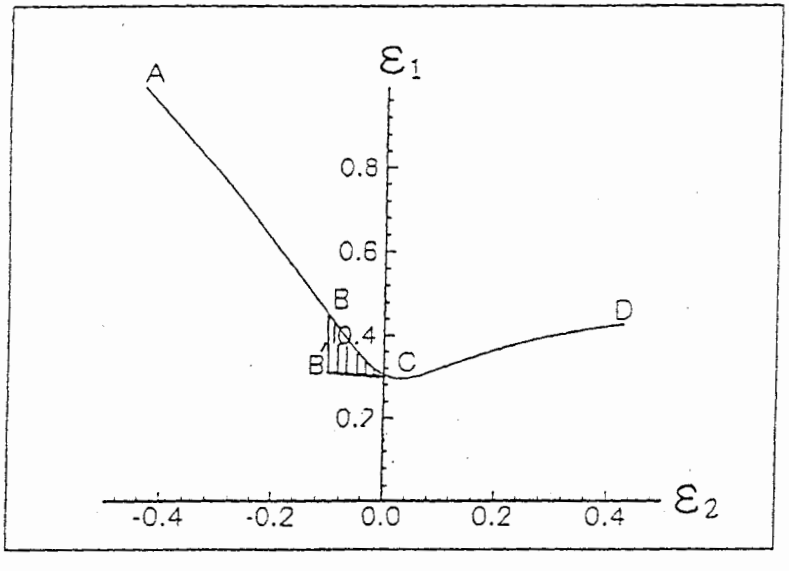

Figure 6: Modified FLD of ST12 sheet respect to strain path in cup drawing

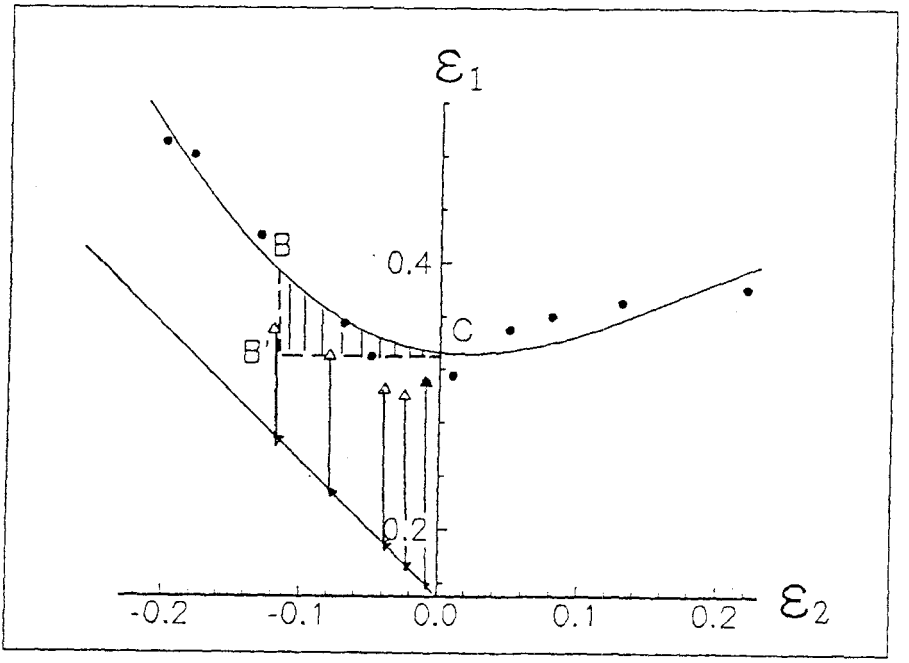

Figure 7: Limits strain in punch radius region : • experimental in linear strain path --- theoretical in actual strain path △ experimental in actual strain path

5 Conclusion

This work provides an experimental and theoretical analysis for the determination of FLD in the actual strain path. The main achievements of this research can be listed as follows:

-Forming limit diagram of the sheets is sensitive to strain path and using the FLD that is obtained in linear strain path for predicting the forming process with non linear strain path will not be accurate.

-The actual limit strains in cup drawing near punch radius region are lower than obtained by FLD that is obtained in linear strain path.

-The theoretical results have good agreements with experiments results.

References

[1] Keeler, S.P. Determination of forming limits in automotive stamping. *Sheet metal Ind.* ,**42** , pp.683-690, 1965.

[2] Goodwin, G.M. Application of strain analysis to sheet metal forming problems in the press shop. *SAE Trans.*, 77, pp. 380 – 387, 1968.

[3] Marciniak, Z., & kuczynski, K. Limit strain in the processes of of stretch – forming sheet metal. *Int., J.Mech.Sci.*, 9 , pp. 609-620, 1967.

[4] Ghosh, A.K. , & Hecker, S.S. Failure in thin sheets stretched over rigid punches. *Met. Trans.* , **6A** , pp. 1065-1071, 1975.

[5] Priadi, D., Magny, C., Massoni, E., Levaillant, C. & Penazzi, L. A new tensile test on notched specimens to assess the forming limit diagram of sheet metals. *J. Mat. Process. Tech.* , **32,** pp. 279-288, 1992.

[6] Pishbin, H., & Gillis, P. Forming limit diagrams calculated using Hill's nonquadratic yield criterion. *Metallurgical. Trans. A* , **23A,** pp.2817.2831, 1992.

[7] Sing, W. M. , & Rao, K. P. Prediction of sheet metal formability using tensile test results. *J. Mat. Process. Tech.* , **37**, pp.37-51, 1993.

[8] Sing, W. M. , & Rao, K. P. Influence of material properties on sheet metal formability limits. *J. Mat. Process. Tech.* , **48**, pp. 35-41, 1995.

[9] Ghosh, A. K. The influence of strain hardening and strain rate sensitivity on sheet metal forming. *Trans. ASME* , **July**, pp. 264-274, 1977.

[10] Burford, D. A. , & Narasimhan, K. A theoretical sensitivity analysis for full-dome formability tests; parameter study for n, m, r and μ. *Metallurgical. Trans. A* , **22A**, pp. 1775-1788, 1991.

[11] Sadough, A. Shakeri, M. & Dariani, B. M. Theoretical and experimental analysis of sheet metal fomability limits. *La Revue de Metallurgie, **May,*** pp. 663-669, 2000.

[12] Sadough, A. Shakeri, M. , & Dariani, B. M. Influence of grain refine annealing on the low carbon steel formability limits. *Proc. Of 98 Asian Conf. On the Heat Treatment of Material* , pp.193-198, 1998.

[13] Kohara, S. Forming limit curves of aluminum and aluminum alloy sheets and effects of strain path on the currves. *J. Mater. Processing Tech. **38,*** pp. 723-735, 1993.

[14] Graf, A., & Hosford, W. Effect of changing strain paths on forming limit diagrams of Al 2008- T4. *Metall Trans. A.,* **24,** pp. 2503-2511, 1993.

[15] Shakeri, M., Sadough, A., & Dariani, B. M. Effect of pre- straining and grain size on the limit strains in sheet metal forming. *Proc Instn Mech Engrs part* B *(ImechE), **214***, pp.821-827, 2000.